Relaxation of 29-cm^{-1} phonons in ruby

R. J. G. Goossens,* J. I. Dijkhuis, and H. W. de Wijn
Fysisch Laboratorium, Rijksuniversiteit Utrecht, P.O. Box 80 000, 3508 TA Utrecht, The Netherlands
(Received 3 April 1985)

The relaxation of resonant 29-cm^{-1} phonons trapped in a laser-excited cylinder of submillimeter diameter is investigated under the conditions of modulated pumping in ruby of 130, 700, and 2500 at. ppm Cr^{3+} at 1.5 K. The decay time T_{eff} of the $2\bar{A}(^2E)$ population, which is a measure of the phonon relaxation time, appears to depend on the metastable population N^* and the cylinder diameter L as the product N^*L only, establishing boundary-limited phonon decay. At N^*L below 5×10^{15} cm^{-2}, pure spatial diffusion prevails. At higher N^*L, where the measured T_{eff} levels off at about 1 μs, dependent on the ground-state concentration, the phonon relaxation is adequately accounted for by the assumption of enhancement by mediation of frequency-shifting Orbach processes at metastable Cr^{3+} subject to diagonal exchange with ground-state Cr^{3+}. Shifts away from resonance to the extent that the phonons escape the zone by ballistic flight are considered active, which predominantly involve distant Cr^{3+} neighbors. Furthermore, a random distribution of Cr^{3+} is assumed, while the exchange is calibrated with reference to pair spectra. The spin-nonflip transitions of metastable Cr^{3+} that are part of the pairs remain at resonance with the phonons because the exchange splittings of $\bar{E}(^2E)$ and $2\bar{A}(^2E)$ are comparable. This is borne out by a separate calculation based on a perturbative molecular field. In addition, experiments have been performed as a function of an external magnetic field up to 4 T parallel to the c axis to disclose the effects of successive separation of the spin-flip and spin-nonflip transitions. The resultant complex development of T_{eff} with field as well as similar data on the R_2 luminescent intensity taken with continuous optical pumping are consistent with exchange-invoked relaxation and, further, yield effective spectral widths of the 29-cm^{-1} transitions of the weakly coupled metastable Cr^{3+} of order 1 cm^{-1}.

I. INTRODUCTION

The problem of the decay of 29-cm^{-1} phonons resonantly trapped by optically excited Cr^{3+} in Al_2O_3 (ruby) has a long history. The earliest indications for remarkable longevity of these phonons came from the observation of a speeding up of the Orbach relaxation within the Kramers doublet $\bar{E}(^2E)$ at 4.2 K.[1] The first actual determination of the lifetime was provided by experiments demonstrating the feasibility of optical detection of nonequilibrium 29-cm^{-1} phonons injected into a ruby crystal with heat pulses.[2] In fact, the lifetime can be derived directly, at least in the case of sufficiently high excited-state concentrations N^* and negligible thermalization, from the decay time of the population of the $2\bar{A}(^2E)$ level. The latter may in turn be registered by means of the R_2 luminescence. These experiments, as well as later ones that also employed optical techniques to generate the resonant phonons,[3,4] all pointed to lifetimes of the order of 1 μs in dilute ruby and a slowing down of the relaxation of $2\bar{A}(^2E)$ with increasing N^*. Of even more interest, the rise of the relaxation time of $2\bar{A}(^2E)$ was found to saturate at high N^*.[5] The role of the metastable Cr^{3+} in the resonant trapping was most strikingly seen by introducing, in a ruby crystal, an additional illuminated region, which acted as an absorptive filter in the flight path from a pulsed heater to the optical-detection volume located at a depth of several millimeters.[6] The occurrence of spectral diffusion at high N^* was first demonstrated by experiments with continuous optical pumping, in which the width of the nonthermal 29-cm^{-1} phonon spike was determined by gradually separating the four Zeeman components of the $\bar{E}(^2E)$-$2\bar{A}(^2E)$ transition in a magnetic field.[7] At low N^* the resonant width is 0.017 cm^{-1}. Continuous experiments have also shown that nearly pure spatial diffusion towards inactive parts of the crystal governs the phonon loss at low N^*.[8] Experiments under the conditions of stationary optical pumping, however, turned out not to be well suited for the determination of relaxation times as such because Raman transitions invoked by the optical-pumping process may severely enhance the $2\bar{A}(^2E)$ population.[9–11] Far-infrared techniques have been used to probe the width of the transition[12] and, among other things, show an accelerated decay induced by x-ray-generated centers.[13] Summarizing the experimental material, we may say, as discussed in greater detail in Sec. III A, that (i) at low N^* the relaxation of 29-cm^{-1} phonons is exclusively determined by spatial diffusion, (ii) at high N^* additional scattering processes involving the excited Cr^{3+} and invoking a modification of the phonon frequency become operative, and (iii) in the optically active zone anharmonic processes are irrelevant.

The experiments presented in this paper examine the 29-cm^{-1}phonon relaxation time, as derived from the decay of the R_2 luminescence upon removal of the pumping, over a wide range of N^* and typical dimensions L of the excited zone and, to some extent, as a function of the ground-state concentration. The saturating behavior is confirmed. An important new result, however, is that within the experimental errors the relevant quantity of the

problem is the product N^*L. The method is time resolved, but, contrary to the case of pulsed excitation, prepares N^* in a quasiequilibrium situation, allowing repetitive scanning at high rates and thereby smaller disturbances. Crucial information is further retrieved from the complex development of the relaxation time with increasing magnetic field, which provides a critical test of the way the various phonon packets communicate. These findings are also related to similar data taken under the conditions of stationary pumping.

As regards the theory, first the inadequacy of existing models is discussed on the basis of the available experimental material. Subsequently, a model is developed that accounts for the lifetime as well as its saturation at high N^* and the magnetic field dependence upon inserting realistic values for the parameters. The model relies on the spectral shift invoked by one-site Orbach processes among the $\bar{E}(^2E)$ and $2\bar{A}(^2E)$ levels of optically excited Cr^{3+} in the static exchange fields of nearby Cr^{3+} in the ground state. (The mechanism of spectral shifting by one-site Orbach processes has earlier been discussed in Ref. 7.) These shifts are, of course, distributed according to the distribution of the exchange parameters. Only if the phonon frequency is moved sufficiently far out into the wings of the transition for the mean free path to exceed L will a wipeout of the phonon occur. As it turns out, spectral shifts invoked by transitions at weakly-exchange-coupled Cr^{3+} sites are already sufficient.

II. EXPERIMENTAL DETAILS

To measure the relaxation time associated with the direct decay of $2\bar{A}(^2E)$ to $\bar{E}(^2E)$, we observed the temporal decay of the R_2 luminescence, emanating from $2\bar{A}(^2E)$, following the switching off of the optical feeding into the broadbands. The relaxation times were measured as a function of the metastable concentration, as determined from the R_1 luminescence intensity, the dimensions of the excited zone, and the Zeeman splittings. The optical excitation was accomplished with an argon laser operating at 514 nm with a maximum power of 2 W. To achieve the required switching speed, the laser beam was focused on an Isomet 1250C acousto-optical modulator deflecting the beam through an aperture in the on period. Rise and fall times better than 30 ns were obtained in combination with repetition rates up to 200 kHz. The luminescence intensities of the R_1 and R_2 lines were measured at right angles to the incident laser beam with a 0.85-m double monochromator followed by standard photon-counting equipment. Sufficient time resolution was provided by a time-to-amplitude converter synchronized to the acousto-optical modulator, in conjunction with a multichannel analyzer operating in the pulse-height-analysis mode. Appropriate corrections to the measured decays were carried out to account for the dead time at higher counting rates.[14] The decays of the R_2 intensity, monitored over at least three $1/e$ periods, were analyzed using the program DISCRETE.[15] They generally appeared to be uniexponential within statistical errors (confidence level greater than 95%). In case of decay times below 80 ns, however, small systematic deviations were observed associated with the finite rise and fall times of the modulator.

The measurements were performed on three different ruby samples. According to atomic-absorption spectroscopy, these samples contained 130, 700, and 2500 at. ppm Cr^{3+}. The samples were the same as the ones used in Refs. 8 and 10. Magnetic susceptibility measurements on all three crystals, however, indicated that these values may systematically be too high by 20%. The samples have the form of thin slabs (thickness 0.3, 0.4, and 0.2 mm, respectively) to ensure sufficient refrigeration in liquid helium at 1.5 K. As to the geometry, the c axis lies in the slab, while the laser beam was incident perpendicular to the slab and polarized parallel to the c axis; the magnetic fields were applied parallel to the c axis.

III. MECHANISMS FOR THE DECAY OF 29-cm^{-1} PHONONS

A. Existing models

In the analysis of the earliest experiments, where 29-cm^{-1} phonons were generated by heat pulses as part of a broad spectrum, anharmonic breakup was assumed to limit the phonon lifetime. Imprisonment in the excited volume, i.e., a diffusive motion from one metastable Cr^{3+} to another to such an extent that the boundary cannot be reached prior to anharmonic decay, then implies a linear increase of the effective relaxation time of $2\bar{A}(^2E)$, T_{eff}, with the metastable concentration N^*. Indeed, a linear N^* dependence has been observed in a number of experiments, resulting in estimates for the phonon lifetime ranging from 0.35 to 1.5 μs.[2–4,16] Substantial support for this was provided by the classical theoretical work of Klemens,[17] which yielded decay times of the order of 1 μs at these frequencies. In later experiments, carried out up to higher N^*, however, T_{eff} was found to flatten out at about 3 μs,[5] pointing to a component of the phonon loss at least proportional to N^*. A further argument against a phonon lifetime limited by anharmonic decay is the observation of a size dependence of T_{eff} (Ref. 5 and Sec. IV below). Similar considerations hold for inelastic impurity scattering.[13]

At least at low N^* and small excited-zone dimensions ($N^*R^2 < 10^{14}$ cm^{-1}), where the trapping of the resonant phonons is not yet complete, spatial diffusion itself is the most efficient decay mechanism.[8] Experimental evidence for this decay mechanism has been provided by the quadratic dependence on N^* of the bottlenecking factor, as deduced from the R_2-R_1 intensity ratio under the condition of continuous pumping.[18] At higher N^* pure spatial diffusion becomes too slow, and processes that involve a change of the phonon frequency out of resonance take over (width of the transition $\Delta\nu \sim 0.02$ cm^{-1}). These processes may, by the amount of the shift, be separated into spectral diffusion and one-step wipeout. In the case of the former mechanism, the shift of the phonon frequency per interruption by an optically excited Cr^{3+} ion is substantially smaller than the width of the transition, and many interruptions are needed before escape via the wings takes place. The shift is provided by a spin-nonflip transition from $\bar{E}(^2E)$ to $2\bar{A}(^2E)$ followed by a spin-flip transition

back to $\bar{E}(^2E)$, or vice versa, and thus equals the random splitting of the $\bar{E}(^2E)$ state by the dipolar interaction or the exchange with distant Cr^{3+} neighbors. Experimental proof that spectral diffusion occurs is found in the broadening of the bottlenecked phonon packet with increasing N^* as observed via the magnetic field dependence of the R_2 intensity,[7,8] but, as it turns out, for the decay of the 29-cm^{-1} phonons the one-step spectral wipeout is more efficient.

The first to suggest a mechanism for spectral wipeout were Meltzer *et al.*,[5] who applied the concepts of resonant two-phonon-assisted energy transfer introduced by Holstein *et al.*[19] to the case of ruby. Here, the electronic energy of an optically excited Cr^{3+} ion is transferred to a Cr^{3+} ion in the $^4A_2$ ground state, with which it is coupled via off-diagonal exchange. The outgoing phonon is shifted in energy by an amount equal to the difference in the optical excitation energy $^4A_2$-$\bar{E}(^2E)$ due to microscopic broadening ($\sim$0.1 cm^{-1}), possibly augmented with the 0.38-cm^{-1} ground-state splitting. The number of active pairs is, of course, proportional to N^*, and accordingly the model correctly predicts a saturation of T_{eff} at high N^*. The model further accounts for the observed inverse proportionality of the saturation value of T_{eff} with the ground-state concentration. Despite these accomplishments, the model is only able to predict the correct T_{eff} if values for the ^2E-$^4A_2$ exchange are taken that are 1—2 orders of magnitude smaller than realistic ones.[20,21] This may be due to the necessary simplifications in the mathematics, as the authors indicate, but it is more likely that a shift of the order of 0.1 cm^{-1} is not sufficient to constitute a one-step wipeout. Reabsorption of the shifted phonons, which is ignored in Ref. 5, presumably is significant because at realistic values of the exchange, whether off-diagonal or diagonal, the mean free path is smaller than the characteristic dimensions of the excited zone. Reabsorption is explicitly taken into account in Sec. III B. Furthermore, the approach of Ref. 5 cannot plausibly explain our observations in Sec. IV of a strong initial fall with an external magnetic field of both T_{eff} and the R_2 intensity. In any case, however, the experimental results by Meltzer *et al.* point to the involvement of Cr^{3+} pairs.

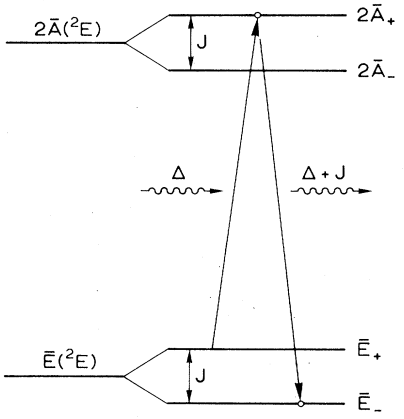

FIG. 1. Frequency-shifting mechanism of resonant phonons involving scattering by an exchange-coupled Cr^{3+} in the excited $\bar{E}(^2E)$ state. The incoming phonon has energy Δ equal to the $\bar{E}(^2E)$-$2\bar{A}(^2E)$ separation (29 cm^{-1}); the outgoing phonon has an energy displaced by J. The analogous process $\bar{E}_- \rightarrow 2\bar{A}_- \rightarrow \bar{E}_+$ modifies the phonon energy by $-J$.

In new experiments on phonon-induced luminescence of fourth-nearest-neighbor N_2 pairs, Basun *et al.*[22] showed that 29-cm^{-1} phonons emitted by isolated Cr^{3+} strongly communicate with transitions within the optically excited pair levels. These transitions occur at 28.5, 28.8, and 29.5 cm^{-1}, and the authors thus concluded that spectral diffusion of the kind discussed above[7] is able to bridge an energy mismatch as large as 0.5 cm^{-1}. They further proposed that the wipeout is furnished by inelastic Orbach processes within the pair levels. These experiments were carried out in heavily doped ruby (0.5 at.% Cr^{3+}), and the results probably are not applicable to more dilute samples. Furthermore, as we will discuss in Sec. III B, the weakly coupled distant Cr^{3+} pairs themselves will provide the spectral diffusion and the wipeout.

B. Inelastic scattering by weakly coupled Cr^{3+} pairs

In this section we present a model for the relaxation of resonant 29-cm^{-1} phonons in ruby. The basis assumptions of the model are the following: (i) A spin-nonflip transition $\bar{E}(^2E)$ to $2\bar{A}(^2E)$ followed by a spin-flip transition back to $\bar{E}(^2E)$ invokes a frequency shift of the resonant 29-cm^{-1} phonons if the metastable Cr^{3+} involved is coupled to a Cr^{3+} in the $^4A_2$ ground state by the *diagonal* part of the exchange (Fig. 1); (ii) the shifted phonons are wiped out, i.e., do not interact with the Cr^{3+} in the optically excited zone, if the shift is sufficiently large for their mean free path to exceed the typical dimension of the zone. The shifts required appear to be of order 1 cm^{-1} or smaller, implying the more distant pairs provide the shifting mechanism. This also allows one to treat the exchange as a molecular field acting on the metastable Cr^{3+}. For reasons of tractibility, no distinction will be made between the substates of $^4A_2$, making the exchange parameter an effective one. The model turns out to explain the flattening out observed at high N^*, the dependence on the Cr^{3+} concentration, and the size dependence. The model also accounts for the speeding up and subsequent slowing down of the relaxation in a magnetic field at high N^*.

We first consider in more detail which Cr^{3+} pairs contribute to the relaxation. It is important to note that the exchange interaction of an optically excited Cr^{3+} with another Cr^{3+} does not notably affect the spin-nonflip frequencies between $\bar{E}(^2E)$ and $2\bar{A}(^2E)$, at least for not too strongly coupled pairs. This point has been relegated to an appendix, in which the effects of a perturbative molecular field are calculated up to third order, yielding the conclusion that the exchange splittings of $\bar{E}(^2E)$ and $2\bar{A}(^2E)$ are equal to the free-electron splitting within a few parts in 10^4. As to the decrease of the exchange interaction J between an optically excited Cr^{3+} and a Cr^{3+} in the $^4A_2$ ground state with increasing distance r, two possible dependences are taken into consideration, viz.,

$$J = J_0 \exp(-ar) \tag{1a}$$

and

$$J = Ar^{-10} . \tag{1b}$$

No experimental results for J are available, but it is not anticipated to differ substantially from the exchange constant between Cr^{3+} in the ground state.[23] In the latter case the exchange has been deduced from pair spectra combined with theoretical considerations,[24] with the result of a ground-state J amounting to about 10 cm^{-1} for fourth-nearest-neighbor pairs at $r = 3.5$ Å. Taking $a = 1$ $Å^{-1}$,[25] we then have $J_0 \approx 330$ cm^{-1}. The pair spectra may similarly be used to calibrate the constant A. At Cr^{3+}-Cr^{3+} separations up to about 10 Å, therefore, the exchange splittings of $\bar{E}(^2E)$ and $2\bar{A}(^2E)$ are larger than the full width of the $\bar{E}(^2E)$ to $2\bar{A}(^2E)$ transition (~ 0.02 cm^{-1}). This, however, is not yet a criterion for a wipeout to take place because phonons having frequencies in the wings of the single-ion resonance line are subject to reabsorption by weakly coupled optically excited Cr^{3+} ions in spin-flip transitions. The mean free path of a phonon shifted from the single-ion resonance by J, either to lower or higher frequency, in fact, equals

$$\Lambda = \frac{2\rho T_d^{(f)}}{D_J N^*} v , \tag{2}$$

in which ρ is the density of phonon states per unit of frequency, $D_J N^*$ is the density of excited Cr^{3+} pairs per unit of frequency, $T_d^{(f)}$ is the spontaneous spin-flip transition time of $2\bar{A}(^2E)$ to $\bar{E}(^2E)$, and v is the velocity of sound. On the assumption that the Cr^{3+} ions are distributed randomly, the probability function of finding the nearest Cr^{3+} at a distance r is given by[25]

$$P(r) = 4\pi N_0 r^2 \exp(-\tfrac{4}{3}\pi N_0 r^3) , \tag{3}$$

in which N_0 is the concentration of Cr^{3+} ions. Inserting Eqs. (1a) and (1b), we then find, for the distribution of the exchange,

$$D_J = \frac{4\pi N_0 [\ln(J/J_0)]^2}{a^3 J} \exp\left[\frac{4\pi N_0 [\ln(J/J_0)]^3}{3a^3}\right] , \tag{4a}$$

and

$$D_J = \frac{4\pi N_0 A^{3/10} J^{-13/10}}{10} \exp(-\tfrac{4}{3}\pi N_0 A^{3/10} J^{-3/10}) , \tag{4b}$$

respectively. For the exponential dependence, this distribution is plotted in Fig. 2. The criterion for wipeout according to assumption (ii) above now simply reads

$$\Lambda \geq L , \tag{5}$$

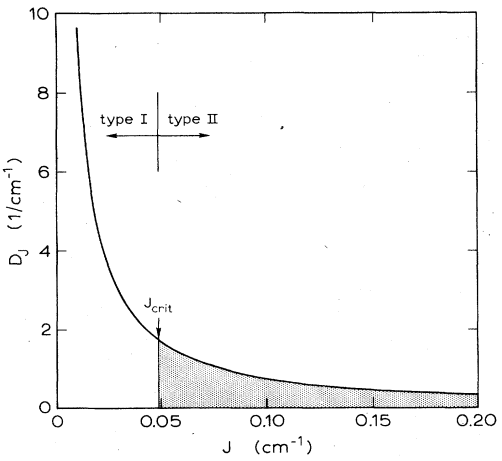

FIG. 2. Distribution of the exchange D_J in the case of exponential dependence of the exchange on distance ($J_0 = 330$ cm^{-1} and $a = 1.0$ $Å^{-1}$) for a Cr^{3+} ground-state concentration of 2500 at. ppm. Optically excited Cr^{3+} experiencing an exchange larger than J_{crit} (type II) are active in wipeout of resonant phonons. The J_{crit} indicated corresponds to $N^* = 10^{18}$ cm^{-3} and $L = 200$ μm.

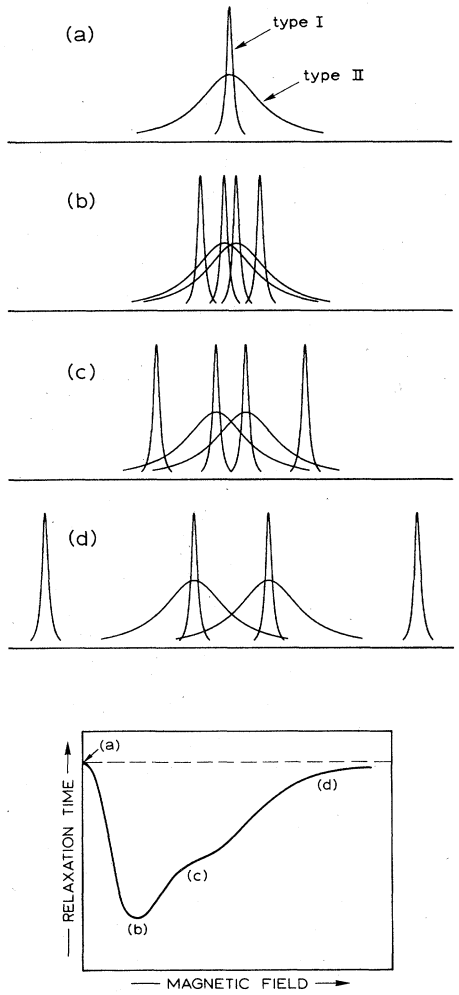

FIG. 3. The upper part is a schematic representation of the position of the resonances of type-I and type-II Cr^{3+} with increasing separation in a magnetic field. The inner type-I resonances are spin-nonflip, the outer ones spin-flip. Transitions of the type-II resonances are spin-nonflip; spinflip transitions are not shown. The lower part depicts resultant development of the relaxation time of $2\bar{A}(^2E)$ in a magnetic field. Labels correspond to the situations depicted in the upper part.

in which L is the average flight path out of the zone. We have $T_d^{(f)}=12$ ns. For 29-cm^{-1} transverse phonons $v=6.4\times10^5$ cm s^{-1},[26] and $\rho=7.3\times10^7$ Hz^{-1} cm^{-3} for the two branches combined, according to Debye. For a typical $N^*=10^{18}$ cm^{-3} and $L=200$ μm, we thus find, from Eqs. (2) and (5), $D_J\leq5.7\times10^{-11}$ Hz^{-1}. In the case of the exponential dependence of $J(r)$ and a ground-state concentration of 2500 at. ppm Cr^{3+}, this corresponds to a "critical" exchange $J_{\rm crit}=0.05$ cm^{-1}, already 3 times the width of the transition (Fig. 2). A particular point to note here is that the relaxation is also effected by the more distant weakly coupled pairs. In our specific example, $J_{\rm crit}$ corresponds to a Cr^{3+} distance of 9 Å [cf. Eq. (1a)]. Integrating D_J over all frequencies larger than $J_{\rm crit}/h$, we find, for the fraction of optically excited Cr^{3+} that are active in a wipeout,

$$\frac{N^{\rm II}}{N^*}=1-\exp\left[\frac{4\pi N_0[\ln(J_{\rm crit}/J_0)]^3}{3a^3}\right], \tag{6a}$$

$$\frac{N^{\rm II}}{N^*}=1-\exp(-\tfrac{4}{3}\pi N_0 A^{3/10}J_{\rm crit}^{-3/10}). \tag{6b}$$

To calculate $T_{\rm eff}$, we write the rate equations for the occupation number p of the resonant 29-cm^{-1} phonons, and the associated rate equations for the $2\bar{A}(^2E)$ populations $N_{2\bar{A}}$ of the Cr^{3+}. The problem is made tractable by dividing the metastable Cr^{3+} into two classes, metastable Cr^{3+} having an exchange splitting below $J_{\rm crit}$ (type I) and those with a larger splitting (type II). In Eqs. (6) we have anticipated this division. Furthermore, the exchange splitting of type I is ignored. (The Zeeman components of type II are denoted by the additional subscripts + and −.) With neglect of other phonon-loss mechanisms and the radiative decay of the metastable population, we then have, in the off period of the optical pumping,

$$\begin{aligned}
\rho\Delta\nu\frac{dp}{dt}&=\frac{(p+1)N^{\rm I}_{2\bar{A}}-pN^{\rm I}_{\bar{E}}}{T_d}\\
&\quad+\alpha\frac{(p+1)(N^{\rm II}_{2\bar{A},+}+N^{\rm II}_{2\bar{A},-})-p(N^{\rm II}_{\bar{E},+}+N^{\rm II}_{\bar{E},-})}{T_d^{(n)}},\\
\frac{dN^{\rm I}_{2\bar{A}}}{dt}&=\frac{-(p+1)N^{\rm I}_{2\bar{A}}+pN^{\rm I}_{\bar{E}}}{T_d},\\
\frac{dN^{\rm II}_{2\bar{A},+}}{dt}&=\alpha\frac{-(p+1)N^{\rm II}_{2\bar{A},+}+pN^{\rm II}_{\bar{E},+}}{T_d^{(n)}}-\alpha\frac{N^{\rm II}_{2\bar{A},+}}{T_d^{(f)}},\\
\frac{dN^{\rm II}_{2\bar{A},-}}{dt}&=\alpha\frac{-(p+1)N^{\rm II}_{2\bar{A},-}+pN^{\rm II}_{\bar{E},-}}{T_d^{(n)}}-\alpha\frac{N^{\rm II}_{2\bar{A},-}}{T_d^{(f)}}.
\end{aligned} \tag{7}$$

Here, the $N_{\bar{E}}$ are the populations of the corresponding $\bar{E}$ levels, $\Delta\nu$ is the width of the resonant phonon packet, $T_d^{(n)}$ and $T_d^{(f)}$ are the spontaneous spin-nonflip and spin-flip transition times of $2\bar{A}(^2E)$ to $\bar{E}(^2E)$, respectively, and

$$1/T_d=1/T_d^{(n)}+1/T_d^{(f)}.$$

The quantity α expresses in a heuristic way a modification of the coupling between the resonant phonons and the type-II Cr^{3+} with reference to type I, evidence for which exists in the magnetic field data below. Note that the last term of the equations for $N^{\rm II}_{2\bar{A},\pm}$ reflects that the shifted phonons produced in the spin-flip decays leave the zone without being reabsorbed. Solving Eqs. (7) under the conditions of strong bottlenecking ($v\rho\Delta\nu T_d/N^*\ll L$), and upon noting that $p\ll1$, $N_{2\bar{A}}\ll N_{\bar{E}}$, and $T_d^{(n)}/T_d\approx1$, we arrive at uniexponential decays of the $2\bar{A}$ populations with the unique decay time

$$T_{\rm eff}=T_d^{(f)}(N^*+\rho\Delta\nu)/\alpha N^{\rm II}, \tag{8}$$

where $N^{\rm II}$ is the total metastable population of type II, already introduced in connection with Eqs. (6), and $N^*=N^{\rm I}+N^{\rm II}$. In case $N^*\gg\rho\Delta\nu\approx4\times10^{16}$ cm^{-3}, $T_{\rm eff}$ thus is inversely proportional to the fraction of optically excited Cr^{3+} with $J>J_{\rm crit}$, as specified by Eqs. (6). Equations (6) contain the N^* and size dependences through $J_{\rm crit}$, and the dependence on the ground-state concentration through N_0 and, to some extent, $J_{\rm crit}$. In the example of above, $N^{\rm II}/N^*$ amounts to 0.27.

Finally, we examine, within the model, the dependence of $T_{\rm eff}$ on a magnetic field parallel to the trigonal axis. A magnetic field splits the energy levels of type-I Cr^{3+}, and introduces further shifts of the already split levels of the type-II Cr^{3+}. The situations arising at various fields are depicted in Fig. 3. It is important to note that the field-induced splitting of type II equals the type-I splitting, i.e., the corresponding spin-nonflip transitions of the two types remain at resonance. The spin-flip resonances for the type-II sites are not considered because of their inherent ineffectiveness for phonon reabsorption. On the grounds of data presented below, we assume that the linewidth of the $\bar{E}(^2E)$-$2\bar{A}(^2E)$ transition of type II is significantly larger than that of type I. In our model this has been incorporated by the factor α. In low magnetic fields [case (b) in Fig. 3], then, the 29-cm^{-1} phonons resonant with type I have become separated into four distinct packets, each of which communicates with as many type-II Cr^{3+} as in the zero-field case [case (a)]. In other terms, the loss per phonon mode has not been modified. The number of participating modes has, however, quadrupled, and accordingly $T_{\rm eff}$ has dropped to one-fourth of its zero-field value.[7] Upon further increase of the field [case (c)], the spin-flip-phonon packets associated with type I become out of resonance with the type-II spin-nonflip transitions. They consequently no longer decay by interaction with type-II Cr^{3+}, but, by scattering with type-I Cr^{3+} under bottlenecking conditions, phonons belonging to the spin-flip and spin-nonflip packets are repeatedly converted into each other. The result is a recovery of $T_{\rm eff}$ by a factor of 2. At very strong fields [case (d)], finally, the energy levels of type II have become distant to the extent that the associated spin-nonflip transitions no longer overlap. As distinct from the previous cases, a spin-nonflip-phonon packet of type I can only be reabsorbed by a single type-II spin-nonflip transition, yielding another factor of 2 of recovery. In summary, $T_{\rm eff}$ versus a magnetic field first falls to one-fourth, and upon further increase of the field returns to the zero-field value. The precise functional dependence of $T_{\rm eff}$, of course, depends on the g factors of $2\bar{A}(^2E)$ and $\bar{E}(^2E)$ and

on the shapes of the transitions and the phonon packets. It is clear, however, that the "half-value" of the initial drop is a measure of the resonant phonon-packet width, while the typical field at which T_{eff} is restoring is a gauge for the type-II transition width.

IV. RESULTS AND DISCUSSION

To examine the N^* and size dependences, we have plotted in Fig. 4, as a function of N^* times the radius R of the excited cylinder, the results of measurements in the 700-at. ppm Cr^{3+} sample. The radius R was controlled by the distance from the focusing lens to the crystal, and varied in the range from 30 to 280 μm. The exciting argon laser was operated in the all-lines modes in order to achieve a detectable R_2 intensity even at low N^* and large R. The N^* were derived from the R_1 intensity and tied to the ground-state concentration by the saturation behavior of R_1 at high pumping.[10] In Fig. 4 T_{eff} was chosen to be plotted versus N^*R to best demonstrate the conformity of our model with both the observed N^* and R dependences. Note here that, according to the model, for the N^* considered ($\rho\Delta\nu \ll N^*$) T_{eff} is inversely proportional to N^{II}/N^*. The latter quantity is in turn determined by J_{crit}, which according to Eqs. (2) and (5) depends on N^* and L in the combination N^*L only, or upon approximating L by R, on N^*R. Indeed, the data in Fig. 4 coincide, within errors, for variations of R over as much as a decade. This observation is of significance to our discussion as it proves quite directly that the energy-shifting mechanism invoking the phonon decay is weak in the sense that only a fraction of the shifts are sufficiently large for the mean free path of the shifted phonons to exceed the zone dimensions.

The solid curve in Fig. 4 represents T_{eff} versus N^*R as calculated from Eq. (8) for the dependence of the exchange according to Eq. (1a). It should be pointed out that the model of Sec. III B allows no adjustment of parameters to be made, except for the multiplicative constant α in the ordinate, which was set to $\alpha=6$ in the case of the exponential dependence of J, and $\alpha=3$ in the case of the r^{-10} dependence. The model of Sec. III B is, in principle, sensitive to the dependence of J on r by the fact that it includes many exchange interactions at various distances, but both dependences considered appeared to track the data with reasonable fidelity. Despite the uncertainties in J versus r, therefore, the model is evidently suited to account for the observed increase of T_{eff}, particularly the flattening off with increasing N^*L. At low N^*L the model overshoots the measured T_{eff}. In this regime, however, there is a significant contribution to the relaxation rate from boundary-limited spatial diffusion of phonons resonant with Cr^{3+} ions of type I. We have[8,27]

$$T_{\text{eff}}^{(\text{dif})} = \frac{3(N^*L)^2}{5.78(v\rho\Delta\nu^{(f)})^2 T_d'} , \tag{9}$$

which in parallel to the model curve for J proportional to e^{-ar} yields the dashed curve in Fig. 4. The time constant T_d' expresses the average coupling of the diffusing phonons with the Cr^{3+} ions of type I and is somewhere intermediate between $T_d^{(f)}=12$ ns and $T_d^{(n)}=1$ ns. We take $T_d'=8$ ns. To establish that boundary-limited spatial diffusion indeed provides a sizable contribution to T_{eff}, we

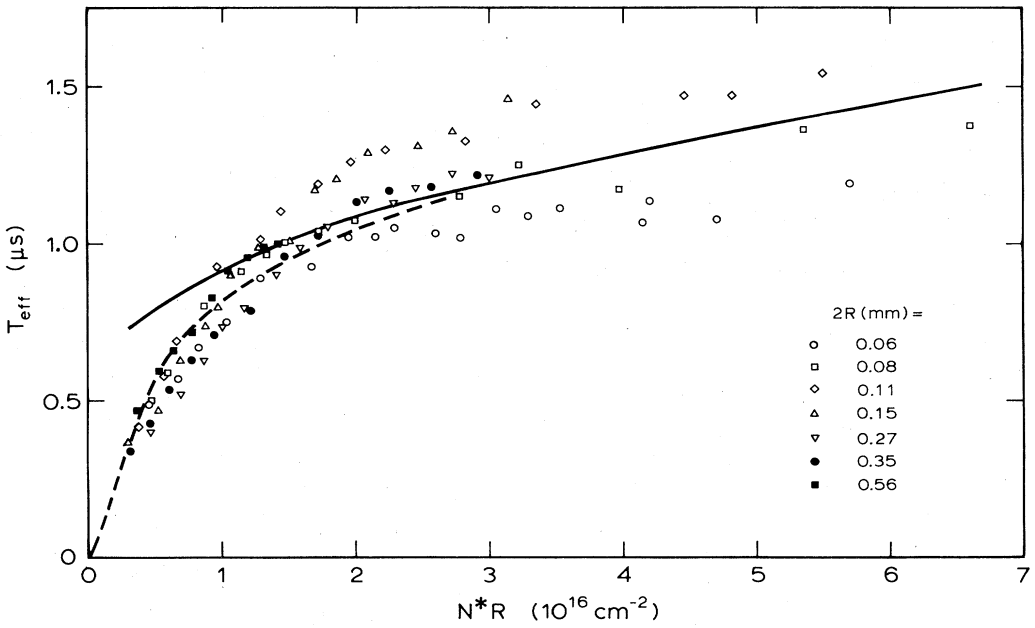

FIG. 4. Effective relaxation T_{eff} of $2\bar{A}(^2E)$ vs N^*R for various diameters $2R$ of the excited zone, as indicated, in ruby with 700 at. ppm Cr^{3+}. The solid line represents T_{eff} due to wipeout of resonant phonons by type-II excited Cr^{3+}, Eq. (8), for the exponential dependence of the exchange on distance, Eq. (1a). The dashed curve includes the additional contribution to T_{eff} of spatial diffusion by type-I Cr^{3+}, as approximated by Eq. (9).

have carried out a separate experiment in the 130-at. ppm Cr^{3+} sample at low N^*, under which conditions spatial diffusion is known to prevail.[8] The results are given in Fig. 5, and confirms that T_{eff} extrapolates to small values at vanishing N^* and varies with N^* faster than linearly.

To investigate the ground-state dependence in some detail, we present T_{eff} as a function of N^* in Fig. 6 for all three samples with the argon laser focused to $R=25$ μm. The data for both 700 and 2500 at. ppm Cr^{3+} are observed to saturate, at 1.1 and 0.6 μs, respectively. (In the 130-at. ppm Cr^{3+} sample leveling off is not reached.) Qualitatively, as anticipated, the saturation value of T_{eff} is lower the higher the ground-state concentration. The observed difference is, however, a factor of 2, while on the basis of Eqs. (6) and (8) T_{eff} at high N^* would differ by a factor of 3.5 for the nominal ground-state concentrations. We consider two possible explanations. First, the Cr^{3+} concentration is known to vary substantially on the scale of the excited zone.[28] Indeed, we have observed T_{eff} in the 700-at. ppm Cr^{3+} sample to vary with the position of the excited cylinder, with values between 0.8 and 2.5 μs. Second, the factor α may differ from sample to sample, and possibly from site to site.

We next turn to the data of T_{eff} of the $2\bar{A}(^2E)$ level as a function of an external magnetic field. In the upper graph of Fig. 7 we have plotted such data, normalized to zero field, in the 2500-at. ppm Cr^{3+} sample at $N^*=4\times10^{18}$ and 3×10^{19} cm^{-3}, and $R=60$ μm. The data at the higher N^* are taken in the regime of full saturation of T_{eff} in zero field, while the data at the lower N^* apply to the onset of saturation. Common to both sets of data points is the fast initial decline of T_{eff}, to approximately 0.4 and 0.25 in the case of the higher and lower N^*, respectively. Next is a slow rise, and, at least for the higher N^*, a full return to unity above 3 T. These experimental features are in general conformity with the predictions of "the model" set forth in Sec. III B (cf. Fig. 3). From the half-value widths of the decline and the subsequent rise, being measures for $\Delta\nu^{I}$ and $\Delta\nu^{II}$, respectively, we estimate $\Delta\nu^{II}$ to be of the order of 1 cm^{-1} and $\Delta\nu^{II}/\Delta\nu^{I}$ of the order of 10; $\Delta\nu^{I}$ has been determined to greater precision than Fig. 7 permits in Ref. 7 with the result $\Delta\nu^{I}\sim0.03$ to 0.2 cm^{-1} at the relevant N^*. Another notable feature of the 2500-at. ppm Cr^{3+} data in Fig. 7, which in fact further substantiates the model of Sec. III B, is a dependence of T_{eff} on the particular Zeeman components of R_2, which in high fields are resolved. Ap-

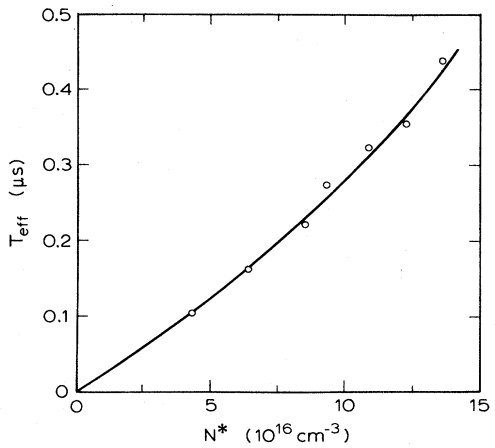

FIG. 5. Effective relaxation time T_{eff} of $2\bar{A}(^2E)$ vs N^* in ruby with 130 at. ppm Cr^{3+}. The excited zone is 400 μm in diameter.

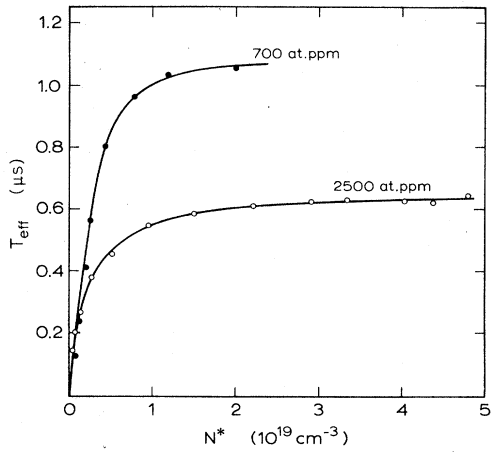

FIG. 6. Effective relaxation time T_{eff} of $2\bar{A}(^2E)$ vs N^* for 700 and 2500 at. ppm Cr^{3+}. The laser beam diameter is 50 μm.

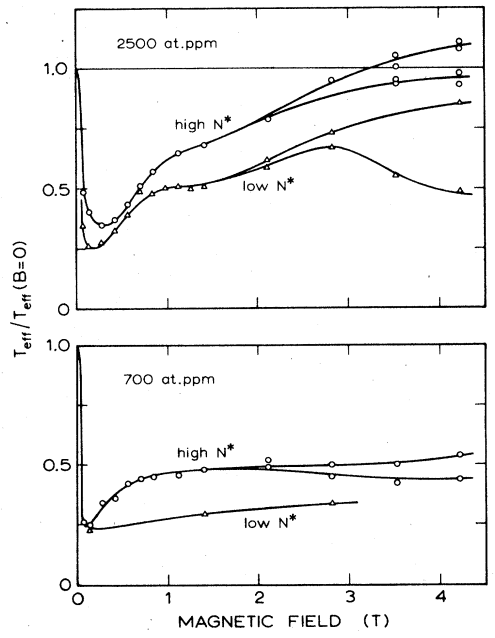

FIG. 7. Effective relaxation time T_{eff} of $2\bar{A}(^2E)$ vs the magnetic field B for 2500 and 700 at. ppm Cr^{3+}. Circles apply to N^* in the regime of dominance of the relaxation by the wipeout process ($N^*\approx3\times10^{19}$ and 6×10^{18} cm^{-3}, respectively); triangles refer to the regime of competition between relaxation by spatial diffusion and type-II wipeout ($N^*\approx4\times10^{18}$ and 2×10^{18} cm^{-3}). The Zeeman components of $2\bar{A}(^2E)$ decay at different rates at the higher fields. The beam diameter is 120 μm.

parently, the $2\overline{A}_+$ level decays slower than $2\overline{A}_-$. This is understood in terms of the model of Sec. III B by observing that in strong fields $\overline{E}_+$ is less populated than $\overline{E}_-$, while a phonon emitted upon relaxation of $2\overline{A}_+$ in a spin-nonflip transition to $\overline{E}_+$ can only be wiped out by a type-II Cr^{3+} in the $\overline{E}_+$ state [cf. Fig. 3, case (d)], and similarly for $2\overline{A}_-$. The population ratio of $\overline{E}_+$ and $\overline{E}_-$ is at very low pumping exclusively determined by the optical feeding, amounting to about 10 in the relevant fields, but gradually reduces to unity at very intense pumping. From the ratio of $T_{\rm eff}$ we deduce an $\overline{E}$ population ratio of 1.2 at the higher N^*, and 1.7 at the lower N^*, in accord with the measured $\overline{E}$ population ratio under similar conditions.[11,29] We finally note in connection with the upper graph of Fig. 7 that the incompleteness of the recovery of $T_{\rm eff}$ at the lower N^* may be attributed to residual spatial diffusion and the modification of $J_{\rm crit}$ upon separating the spin-nonflip transitions of the type-II Cr^{3+}. In Fig. 7 we further present similar data in the 700-at. ppm Cr^{3+} sample for $N^*=2\times10^{18}$ and 6×10^{18} cm^{-3}, and $R=60$ μm. Here, saturation is not fully reached even at the high N^*, which is reflected in only partial recovery of $T_{\rm eff}$ after the initial drop to 0.25. The field splitting of $T_{\rm eff}$ at high fields corresponds to an $\overline{E}_+$ over $\overline{E}_-$ type-II population ratio of 1.2, again consistent with Ref. 29. The low-N^* data exhibit only a marginal increase with field beyond the minimum, indicative of the substantial effects of spatial diffusion in this case.

At this point it is useful to point out that exactly the same information on the $2\overline{A}$ relaxation is contained, although in a less direct way, in the development of the R_2 luminescence intensity with the field in experiments under the conditions of continuous pumping. Such experiments have the considerable advantage that they may cover a larger range of N^*, in particular towards low N^*. The gist of why the continuous scheme and the time-resolved method employed above are equivalent is the elimination by normalizing at zero field of the augmented feeding into $2\overline{A}(^2E)$ due to optically induced Raman processes connecting $\overline{E}(^2E)$ and $2\overline{A}(^2E)$.[9] Experimental confirmation for the equivalence is found in Fig. 8 in which, for ruby with 700 at. ppm Cr^{3+}, both $T_{\rm eff}/T_{\rm eff}(B=0)$ and $R_2/R_2(B=0)$, as measured in a single run, are plotted as a function of B, and at high N^* are seen to coincide within errors. At low N^* ($\sim10^{17}$ cm^{-3}) a systematic departure by a constant factor is observed to occur above 0.1 T. This has to do with the subtle difference of the N^* dependences of $T_{\rm eff}$ and R_2 by a factor $1+\rho\Delta\nu^{\rm I}/N^*$ at $B=0$,[9] increasing to $1+4\rho\Delta\nu^{\rm I}/N^*$ at full separation of the type-I phonon packets. From the experimental

$$[T_{\rm eff}/T_{\rm eff}(B=0)]/[R_2/R_2(B=0)]=1.4\ ,$$

we deduce $\rho\Delta\nu^{\rm I}/N^*=0.15$, yielding with the Debye ρ and $\Delta\nu^{\rm I}=0.02$ cm^{-1} the result $N^*=2.9\times10^{17}$ cm^{-3}, consistent with $N^*=3\times10^{17}$ cm^{-3} according to the independent N^* calibration used here.

Results for $R_2/R_2(B=0)$ in ruby with 2500 at. ppm Cr^{3+} up to 3 T are presented in Fig. 9 for N^* ranging from 5×10^{17} to 8×10^{18} cm^{-3} and $R=60$ μm; similar data in ruby with 700 at. ppm Cr^{3+} for N^* ranging from 2×10^{17} to 5×10^{18} cm^{-3} are presented in Fig. 10. Also in

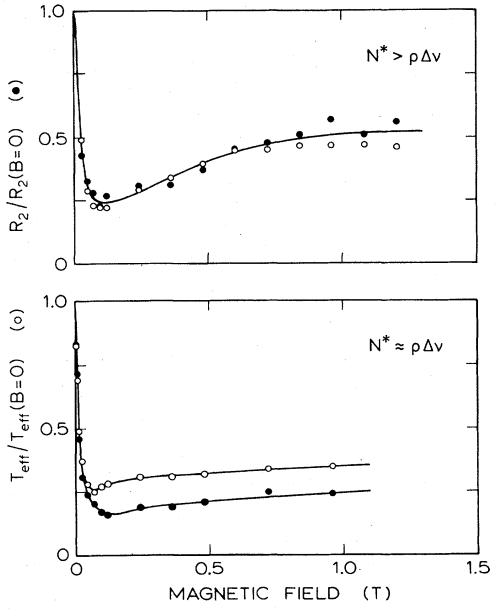

FIG. 8. Field dependence of $T_{\rm eff}$ (open circles) and R_2 (solid circles) in ruby with 700 at. ppm Cr^{3+} for the regimes $N^* > \rho\Delta\nu$ and $N^* \approx \rho\Delta\nu$. These dependences are identical, apart from the factor $1+\rho\Delta\nu/N^*$, as discussed in text. The beam diameter is 120 μm.

Fig. 10 a set of data is inserted for $R=500$ μm and correspondingly reduced N^*, which is indistinguishable from the data for $N^*=2\times10^{17}$ cm^{-3} and $R=60$ μm, indicating negligible dependence of the field dependence on N^*R. The data of Figs. 9 and 10, in general, exhibit the same characteristics as $T_{\rm eff}$. In particular, the 700-

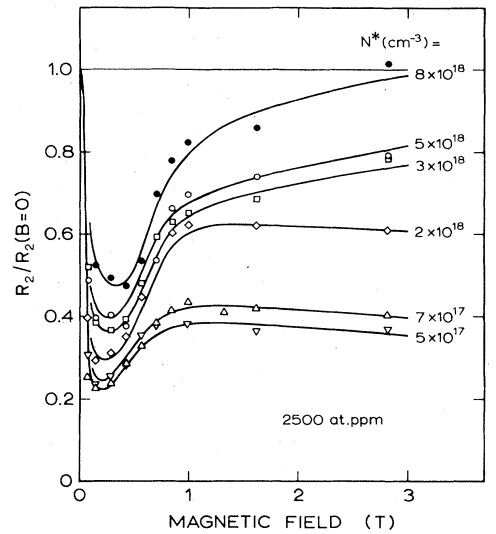

FIG. 9. Field dependence of R_2 in ruby with 2500 at. ppm Cr^{3+} at various N^*. The beam diameter is 120 μm. Data have been corrected for reabsorption by Cr^{3+} in the $^4A_2$ ground state, with account for the transition probabilities of the R_2 Zeeman components and, as a function of the magnetic field, the population distribution of the $^4A_2$ sublevels.

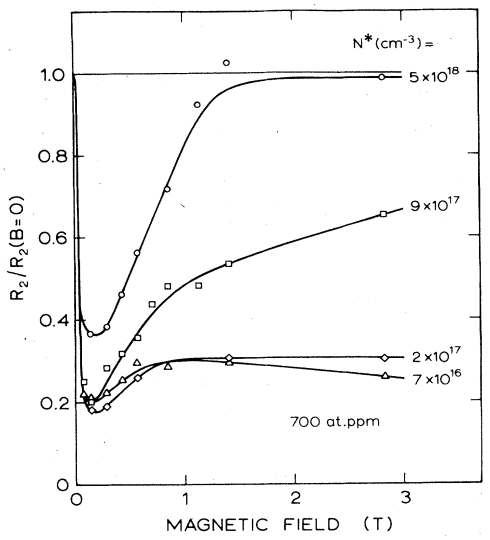

FIG. 10. Same as Fig. 9, but 700 at. ppm Cr^{3+}. The beam diameter is 120 μm, but 1 mm in the case of $N^*=7\times10^{16}$ cm^{-3}. Corrections for reabsorption are minor in this case.

at. ppm Cr^{3+} data show to better advantage than Fig. 6 a full recovery of T_{eff} at fields above 1 T. Figures 9 and 10 further allow a more accurate determination of $\Delta\nu^{\text{II}}$, with the result $\Delta\nu^{\text{II}}=0.7$ cm^{-1} in ruby with 700 at. ppm Cr^{3+} at $N^*\sim10^{19}$ cm^{-3}, and $\Delta\nu^{\text{II}}=1.1$ cm^{-1} in ruby with 2500 at. ppm Cr^{3+} at $N^*=3\times10^{19}$ cm^{-3}. These results for $\Delta\nu^{\text{II}}$ are generally in conformity with the α required in the fitting of T_{eff} to N^*L in Fig. 4. Possible sources for the broadening of the spin-nonflip transitions with decreasing distance are a larger inhomogeneous broadening due to a lowering of the symmetry and crystal deformations, and variations of the $2\bar{A}(^2E)$-$\bar{E}(^2E)$ spin-nonflip separation with anisotropic components of the exchange. Another source would be an increased spin-phonon interaction, which, however, would also affect the quantity α through T_d.

V. CONCLUDING REMARKS

The most important result of this paper is an adequate description of the magnitude of the $2\bar{A}(^2E)$ relaxation, which under bottlenecking conditions is a direct measure of the loss of 29-cm^{-1} phonons, and its dependence on (i) the metastable population, (ii) the dimensions of the excited zone, (iii) the ground-state concentration, and (iv) an external magnetic field. The model developed is based on one-site Orbach processes of Cr^{3+} in exchange fields of nearby Cr^{3+}. A resonant spin-nonflip transition followed by a spin-flip transition brings the phonon excitation out of range in case the outgoing phonon has its frequency shifted into the wings sufficiently far for the mean free path to surpass the zone dimensions. A quantity relevant to the problem then turns out to be the metastable population times the typical zone dimension. The parameters involved, in particular the Cr^{3+}-Cr^{3+} exchange versus distance, are all known from other sources to sufficient precision, with the exception of the widening of the 29-cm^{-1} spin-nonflip transition, here heuristically expressed in the width $\Delta\nu^{\text{II}}$. The latter appears, however, to be in conformity with the development of the $2\bar{A}(^2E)$ relaxation in a magnetic field, and is further supported by spectroscopic evidence for a larger $\Delta\nu$ of weakly coupled pairs in the ground state.[30] Small differences in the exchange splittings of $\bar{E}(^2E)$ and $2\bar{A}(^2E)$ could be responsible for $\Delta\nu^{\text{II}}$. The model underestimates the observed decay rate at small N^*, but here boundary-limited spatial diffusion has become the prevailing decay mechanism. A particular point to note is that the model is consistent with realistic values of the exchange. It incorporates Cr^{3+} interactions over both small and large distances with, for zone dimensions of order 0.1 mm, a critical exchange of order 1 cm^{-1}, above which the one-site Orbach process is taken to result in a phonon loss. The spectroscopic observation of involvement of N_2 pairs,[22] having an exchange of the order of 10 cm^{-1}, thus supports our findings. A model proposed earlier, two-site resonant-phonon-assisted energy transfer,[5] also based on exchange interactions of neighboring Cr^{3+}, could only be made to work by taking the exchange to be reduced by 2 orders of magnitude, but even then does not account for the magnetic field dependence. This reduction is not likely to be true. The energy-transfer process, which, as the present mechanism is physically realistic, presumably is ineffective in causing $2\bar{A}(^2E)$ relaxation because of the absence of microscopic broadening or because it shifts the excitation by such small amounts that the shifted phonon still sees the crystal as being opaque.

ACKNOWLEDGMENTS

The authors are indebted to G. J. Dirksen for crystal growing, C. R. de Kok for technical assistance, and E. H. van Mol for participating in the experiments. Financial support by the Netherlands Foundations Fundamenteel Onderzoek der Materie and Zuiver Wetenschappelijk Onderzoek is acknowledged.

APPENDIX: EXCHANGE SPLITTINGS OF THE $\bar{E}(^2E)$ AND $2\bar{A}(^2E)$ DOUBLETS

We rely, much as Clogston in his calculations of the perpendicular g factor in an external magnetic field,[31] on the method of Sugano *et al.*,[32] i.e., we adopt the cubic-field representation and treat the Coulomb interaction, the spin-orbit interaction, the trigonal field, and, in the present context, the exchange interaction as perturbations. In the calculations all states $|\, n,\gamma,m\,\rangle$ belonging to the t_2^3 and t_2^2e electronic configurations, which number 80 in all, have been considered. The quantum number γ distinguishes within the orbital degeneracy, while m denotes the projection of the spin angular momentum. The energies of these states are taken from a diagonalization of the full 80×80 secular determinant, as carried out by Sugano and

Peter,[33] but with overall corrections to achieve better coincidence with known experimental positions. Of particular interest here are, of course, the four states $|t_2^3\,{}^2E,\gamma,m\rangle$, where $\gamma=u_+,u_-$ and $m=\pm\frac{1}{2}$. In the absence of exchange, these states split in second order by the combined action of the spin-orbit interaction and trigonal field into the two Kramers doublets $\bar{E}(^2E)$ and $2\bar{A}(^2E)$. The upper doublet contains the states $|u_+,+\frac{1}{2}\rangle$ and $|u_-,-\frac{1}{2}\rangle$, while the lower one is comprised of $|u_-,+\frac{1}{2}\rangle$ and $|u_+,-\frac{1}{2}\rangle$. Upon treating the exchange interaction as a molecular field parallel to the trigonal axis, perturbations up to third order need be considered for departures of the g factors from the free-electron $g_e=2.0023$ in spin Hamiltonians of the form $\mathcal{H}=g\mu_B H_{ex}S_z$. Since the exchange is diagonal in the orbital quantum numbers, the relevant chains of matrix elements each involve, although twice, only one other cubic level, and as a result are quite limited in number. In fact, the third-order corrections to the energies of the $t_2^3\,{}^2E$ states linear in H_{ex} turn out to read (see, e.g., Ref. 34 for general perturbation expressions)

$$E_3(t_2^3\,{}^2E,\gamma,m)=g_e\mu_B H_{ex}\sum_{\substack{n',\gamma',m'\\(n'\neq t_2^3\,{}^2E)}}|\langle t_2^3\,{}^2E,\gamma,m\,|\,V\,|\,n'\gamma'm'\rangle|^2(m'-m)/[\Delta E(n')]^2\,, \tag{A1}$$

which is to be compared with the first-order energies $g_e\mu_B H_{ex}m$ (the second-order corrections in H_{ex} vanish). The quantity V represents the perturbation exclusive of the exchange, and the $\Delta E(n')$ denote the zero-order energies of $|n'\rangle$ relative to $|t_2^3\,{}^2E\rangle$. The four states $|t_2^3\,{}^2E,\gamma,m\rangle$ as chosen conform to the requirements for the validity of Eq. (A1) that (i) within these states the total perturbation V is diagonal in first order, and (ii) the second-order corrections to the energies due to V are diagonal within the degeneracy left in first order, i.e., within the subspace spanned by u_+ and u_-. We note, however, that the tables of matrix elements prepared by previous workers[32,33] are expressed in terms of the orbital quantum numbers u and v rather than u_+ and u_-, and therefore need first to be reworked according to the relation $|u_\pm\rangle=2^{-1/2}(|u\rangle\pm i\,|v\rangle)$. A further substantial reduction of the number of matrix-element chains to be evaluated is accomplished by noting that in Eq. (A1) m' must be unequal to m. This eliminates the Coulomb interaction and trigonal field in producing deviations from g_e, leaving the spin-orbit interaction. Evaluating the remaining terms in Eq. (A1), we arrive at the result that up to third order the exchange splittings of $\bar{E}(^2E)$ and $2\bar{A}(^2E)$ are equal, with the g factor

$$g=g_e\{1-\tfrac{2}{3}\zeta^2/[\Delta E(t_2^3\,{}^2T_2)]^2+\tfrac{5}{9}\zeta'^2/[\Delta E(t_2^2(^3T_1)e\,{}^4T_2)]^2-2\zeta'^2/[\Delta E(t_2^2(^1T_2)e\,{}^2T_1)]^2-\tfrac{2}{9}\zeta'^2/[\Delta E(t_2^2(^3T_1)e\,{}^2T_2)]^2\}\,. \tag{A2}$$

Here, ζ is the spin-orbit interaction parameter, and $\zeta'=\zeta(1-\epsilon)^{1/2}$, with ϵ the covalency parameter. Inserting the reasonable estimates $\zeta=170$ cm^{-1} and $\epsilon=0.19$ for the case of ruby,[33] we find $g=g_e(1+4\times10^{-4})$. Contributions to g of fourth and higher order are, of course, anticipated to be even smaller by, say, the trigonal field strength over a typical excitation energy within the cubic levels. The primary contributions proportional to H_{ex}^2 are of fourth order. As a general conclusion we may therefore say that the spin-nonflip separations between $\bar{E}(^2E)$ and $2\bar{A}(^2E)$ stay at resonance with one another, and, for that matter, with an isolated Cr^{3+}, within a few parts in 10^4 of the exchange splittings. This conclusion would not be essentially modified if transverse exchange fields instead of an H_{ex} parallel to the c axis had been considered.

*Present address: Philips Research Laboratories, Eindhoven, The Netherlands.

[1]S. Geschwind, G. E. Devlin, R. L. Cohen, and S. R. Çhinn, Phys. Rev. 137, A1087 (1965); R. Adde, S. Geschwind, and L. R. Walker, in *Proceedings XVth Colloque Ampère,* edited by P. Averbuch (North-Holland, Amsterdam, 1969), p. 460.

[2]K. F. Renk and J. Deisenhofer, Phys. Rev. Lett. **26**, 764 (1971); K. F. Renk and J. Peckenzell, J. Phys. (Paris) Colloq. **33**, C4-103 (1972).

[3]R. S. Meltzer and J. E. Rives, Phys. Rev. Lett. **38**, 421 (1977).

[4]G. Pauli and K. F. Renk, Phys. Lett. **67A**, 410 (1978).

[5]R. S. Meltzer, J. E. Rives, and W. C. Egbert, Phys. Rev. B **25**, 3026 (1982).

[6]A. A. Kaplyanskii, S. A. Basun, V. A. Rachin, and R. A. Titov, Pis'ma Zh. Eksp. Teor. Fiz. **21**, 438 (1975) [JETP Lett. **21**, 200 (1975)].

[7]J. I. Dijkhuis, A. van der Pol, and H. W. de Wijn, Phys. Rev. Lett. **37**, 1554 (1976).

[8]J. I. Dijkhuis and H. W. de Wijn, Phys. Rev. B **20**, 1844 (1979); Solid State Commun. **31**, 39 (1979).

[9]S. A. Basun, A. A. Kaplyanskii, and V. L. Shekhtman, Fiz. Tverd. Tela (Leningrad) **24**, 1913 (1982) [Sov. Phys.—Solid State **24**, 1093 (1982)].

[10]R. J. G. Goossens, J. I. Dijkhuis, and H. W. de Wijn, Phys. Rev. B **32**, 5163 (1985).

[11]J. G. M. van Miltenburg, J. I. Dijkhuis, and H. W. de Wijn (unpublished).

[12]H. Lengfellner, J. Hummel, H. Netter, and K. F. Renk, Opt. Lett. **8**, 220 (1983); N. Retzer, H. Lengfellner, and K. F. Renk, Phys. Lett. **96A**, 487 (1983).

[13]M. Engelhardt and K. F. Renk, in *Proceedings of the Fourth International Conference on Phonon Scattering in Condensed Matter, Stuttgart, 1983,* edited by W. Eisenmenger, K. Lassman, and S. Döttinger (Springer, Berlin, 1984), p. 124.

[14]R. L. McGuire, E. C. Yates, D. G. Crandall, and C. R. Hatcher, IEEE Trans. Nucl. Sci. **NS-12**, 24 (1965); L. M. Bollinger

and G. E. Thomas, Rev. Sci. Instrum. **32**, 1044 (1961).
[15]S. W. Provencher, J. Chem. Phys. **64**, 2772 (1976).
[16]A. A. Kaplyanskii, S. A. Basun, and V. L. Shekhtman, J. Phys. (Paris) Colloq. **42**, C6-439 (1981).
[17]P. G. Klemens, J. Appl. Phys. **38**, 4573 (1967).
[18]The interpretation of these experiments in Ref. 8 is only valid in the regime where direct optical feeding into $2\overline{A}(^2E)$ dominates the Raman processes from $\overline{E}(^2E)$ to $2\overline{A}(^2E)$ invoked by optically generated zone-boundary phonons, i.e., $N^*R < 10^{15}$ cm^{-2} (see, e.g., Ref. 10).
[19]T. Holstein, S. K. Lyo, and R. Orbach, Phys. Rev. Lett. **36**, 891 (1976).
[20]R. J. Birgeneau, J. Chem. Phys. **50**, 4282 (1969).
[21]G. F. Imbush, Phys. Rev. **153**, 326 (1967).
[22]S. A. Basun, A. A. Kaplyanskii, S. P. Feofilov, and V. L. Shekhtman, Fiz. Tverd. Tela (Leningrad) **25**, 2731 (1983) [Sov. Phys.—Solid State **25**, 1570 (1983)].
[23]J. W. Allen, R. M. Macfarlane, and R. L. White, Phys. Rev. **179**, 523 (1969).
[24]L. F. Mollenauer and A. L. Schawlow, Phys. Rev. **168**, 309 (1968).
[25]S. K. Lyo, Phys. Rev. B **3**, 3331 (1971).
[26]B. Taylor, H. J. Maris, and C. Elbaum, Phys. Rev. B **3**, 1462 (1971).
[27]Equation (9) differs from the corresponding expression in Ref. 8 by the factor 5.78 in lieu of 8, which is related to solving the rate equations for T_{eff} under time-resolved conditions instead of for $N_{2\overline{A}}/N_{\overline{E}}$ under stationary conditions.
[28]A. N. Belaya, E. R. Dobrovinskaya, L. A. Litvinov, V. V. Pishshik, A. I. Fisun, and E. I. Chernyakov, Kristallografiya **22**, 411 (1977) [Sov. Phys.—Crystallogr. **22**, 232 (1977)].
[29]J. I. Dijkhuis and H. W. de Wijn, Phys. Rev. B **20**, 3615 (1979).
[30]P. M. Selzer, D. S. Hamilton, and W. M. Yen, Phys. Rev. Lett. **38**, 858 (1977).
[31]A. M. Clogston, Phys. Rev. **188**, 1229 (1960).
[32]S. Sugano, Y. Tanabe, and H. Kamamura, *Multiplets of Transition-Metal Ions in Crystals* (Academic, New York, 1970).
[33]S. Sugano and M. Peter, Phys. Rev. **122**, 381 (1961).
[34]E. V. Condon and G. H. Shortley, *The Theory of Atomic Spectra* (Cambridge University Press, Cambridge, England, 1951), pp. 30ff.